

## JOINT PANEL ZONES AS SEISMIC ENERGY DISSIPATORS IN MOMENT RESISTING FRAMES

Amit Nagar and Challa V.R. Murty  
Department of Civil Engineering  
Indian Institute of Technology Kanpur  
Kanpur - 208016.

### ABSTRACT

Strong seismic ground motions push steel moment resisting frames into states of severe material nonlinearity. A properly designed and detailed frame can exploit the stable hysteretic characteristics of its constituent elements, namely, beam-columns, joint panel zones, walls and slabs, to dissipate the input seismic energy. Of all these elements constituting a frame, the finite-sized joint panel zones possessing finite strength and finite initial stiffness, are ideally suited to perform this task. The paper presents the influence of joint panel zone design on the overall seismic energy dissipation capacity of the frame. A new philosophy for the design of MRF's is proposed for consideration, which may replace the current "Strong Column - Weak Girder" philosophy.

### INTRODUCTION

The most common form of construction of buildings is that of the moment-resisting frame type, wherein a building is composed of linear members (called beam-columns), slabs and walls. A well-designed and constructed moment resisting frame building is expected to behave inelastically under the strong earthquake ground motions, and dissipate the input seismic energy without collapse. This paper addresses the role of frame joints in the dissipation of input seismic energy, and observes that the frame behaviour is also sensitive to the design of beam-column joints. Thus, the joints can be so designed as to improve the hysteretic energy dissipation within the frame. This is demonstrated through the modelling of joints in 2D steel frames.

### MACRO MODELLING OF JOINTS

While modelling buildings, detailed cyclic inelastic constitutive models of each of its components, e.g., beam-columns, joint panel zones, walls and slabs, are required. Modelling of beam-columns is very well discussed in the literature (Chen & Atsuta, 1977; Murty, 1992). Research on modelling walls and slabs is underway. The modelling of joint panel zones alone is discussed here.

### Joint Panel Zones

The terms *panel zone* and *connection* appear often in the literature describing studies associated with junctions of beams and columns. The panel zone, or the *joint*, refers to the finite-sized area at the junction of the beams and the columns, while the connection refers to the means by which the

beams are connected to the columns, e.g., welding and bolting. Nonlinearities in a frame may arise from both joint panels and connections. The nonlinearities due to the flexible joint panel zones alone are discussed here. The connections between the beam-columns and the joint panel zones are assumed to be rigid, and the nonlinearities arising from the connections are negligible.

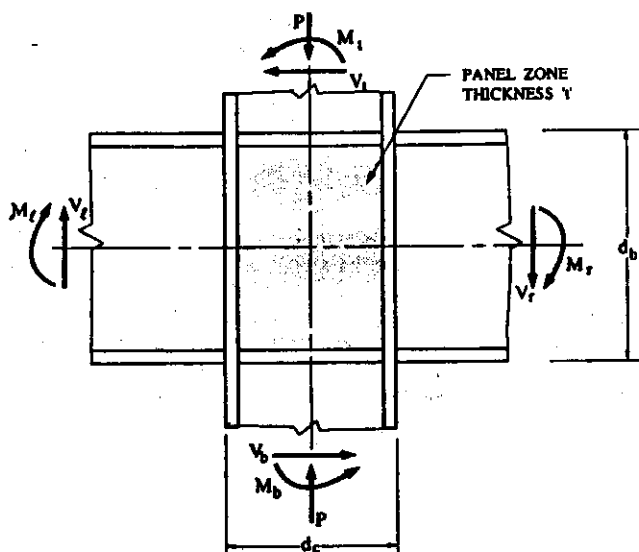


Figure 1 : Geometry and loads transferred through a planar joint.

The lateral resistance of a steel MRF depends on how well the applied loads are transferred between the beams and the columns (see Fig.1); and this is, in fact, decided by the joints. In the early 70's, detailed experimental (Krawinkler *et. al.*, 1971) and numerical (Pinkney, 1973) studies revealed that joints possess highly nonlinear characteristics in the form of large ductilities and good hysteretic properties. It is observed that the joints are stiff axially and flexurally, but flexible in in-plane shear. The high shear forces caused by the unbalance of beam moments result in large joint shear strains affecting the storey-drift and overall frame response.

The primary responsibilities of a frame joint are :

- (1) to resist the interaction of multi-directional forces transferred through it,
- (2) to possess adequate ductility to carry large deformations to facilitate the redistribution of forces in the frame, without any brittle failure in it or without the collapse of the frame, and
- (3) to possess good energy-dissipating qualities.

The analytical modelling of the joints is burdened by their complex construction. The joint panel plate, the flanges of the beams and of the columns, the doubler plates and the web stiffeners enter the load-deformation characteristics together. A clear distinction of the contribution due to each of these is not available due to their strong inter-dependence. However, some researchers have proposed simplified models accounting for one or more of

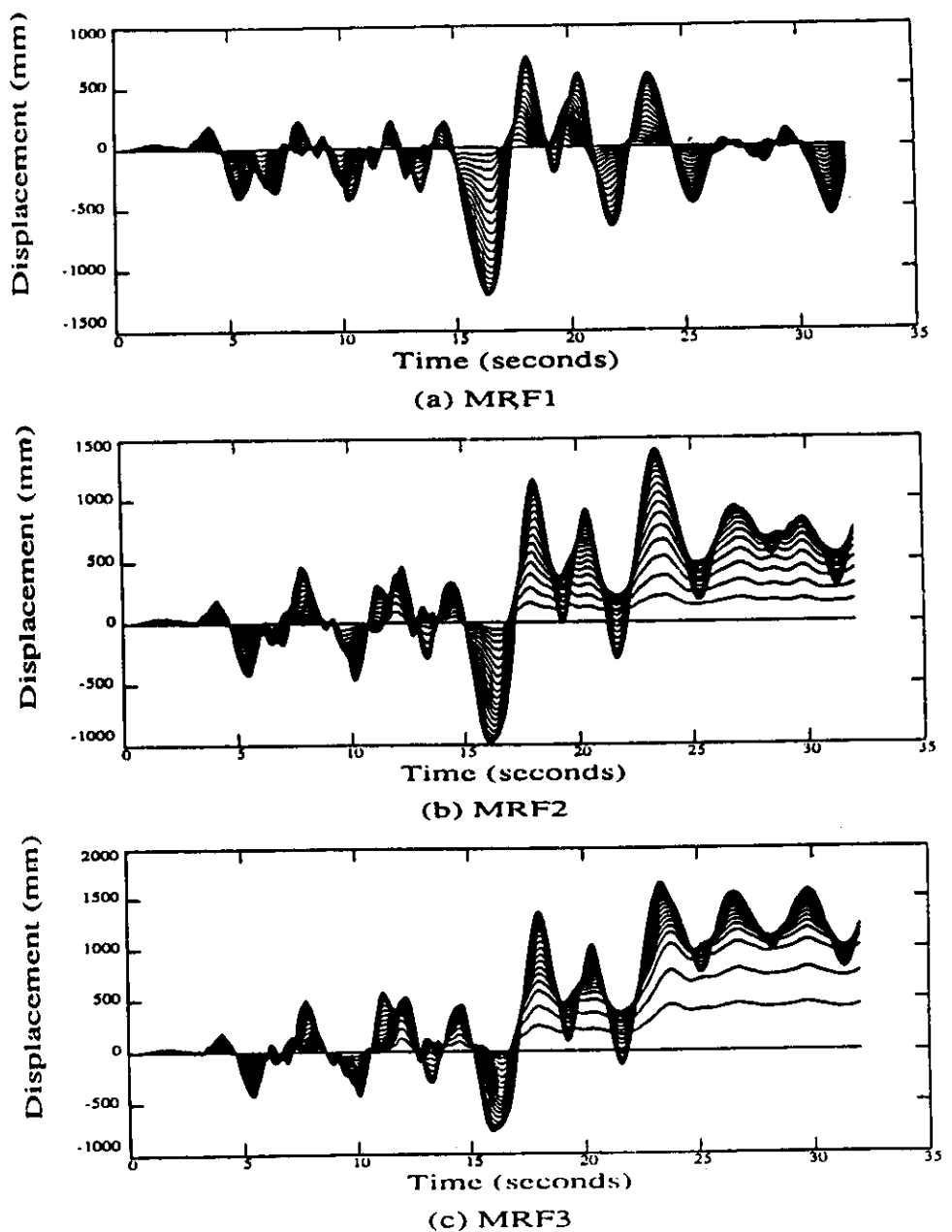


Figure 2 : Influence of different joint designs (J1, J2 and J3) on the lateral displacement time histories of all floors of a twenty storey building (Nakao, 1973). The outermost curves correspond to the roof, and the innermost to the first floor.

these contributions to analytically describe the hysteretic strength and stiffness of joints. Only few of them (Krawinkler *et. al.*, 1975; Kato, 1982; Fielding & Chen, 1973) are valid under cyclic loads.

#### Earlier Joint Panel Zone Models

The joints in a frame were assumed to be rigid in the earlier nonlinear dynamic analysis of frames, until their hysteretic properties were revealed experimentally (Bertero *et. al.*, 1972). For typical code-designed buildings, the joints panels are flexible enough to be included as flexible elements in the analysis of a frame. Further, their yield strength is low enough and they undergo considerable yielding under strong earthquake loads, possibly even before the plastic hinges occur in the beams. The true strength and stiffness of the joints play a very important role in the overall nonlinear behaviour of steel MRF's (Murty, 1992) (see Fig.2). Thus, an adequate mathematical model to analytically describe their nonlinear response is essential for inclusion in realistic frame analyses.

Detailed experimental (Kato, 1982; Bertero, 1972; Becker, 1975) and analytical (Pinkney, 1973; Krawinkler *et. al.*, 1975; Kato, 1982; Fielding & Chen, 1973; Krawinkler, 1978; Tsai & Popov, 1988) studies conducted on beam-column joints in the past two decades resulted in a much better understanding of its hysteretic behaviour. Under large unbalance of beam moments, first the center of the joint reaches yield, and then the yielding propagates towards the edges of the joint panel, resulting in an almost uniform yielded state in the panel (see Fig.3).

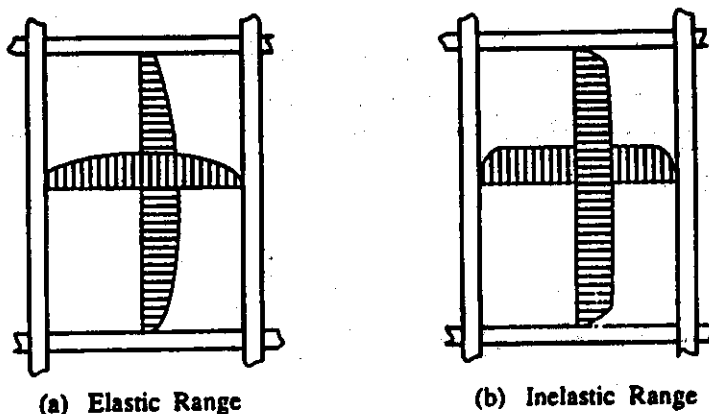
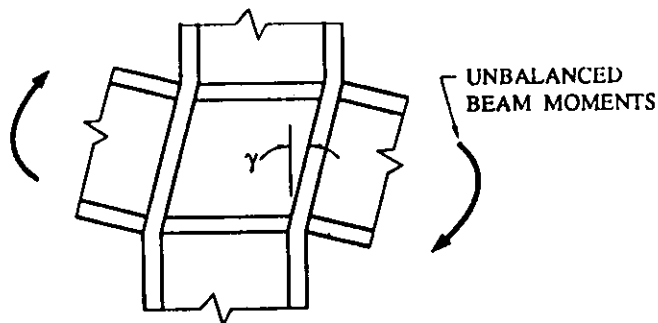
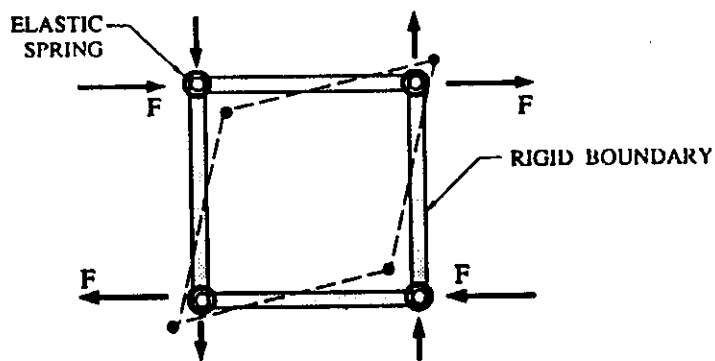


Figure 3 : Shear stress distribution in a planar joint.

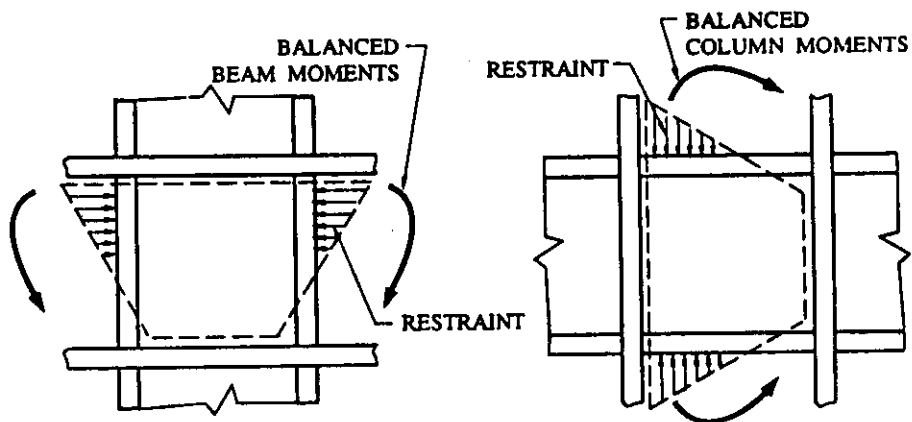
Within the joint panel zone, the column axial force and bending moments are primarily carried by the flanges. The influence of column axial force on the general yielding of the joint is usually small (Nakao, 1973). The primary factors that contribute to the shear stiffness of the joint, are (a) shear resistance of the panel zone plate up to yield (see Fig.4a), (b) resistance of the panel boundary elements (Krawinkler *et. al.*, 1975), i.e., beam and column flanges (see Fig.4b), (c) restraint to the panel zone flexural deformation



(a) Shear Behaviour Caused by Unbalanced Beam Moments



(b) Resistance of the Panel Boundary Elements [16]



(c) Restraint to Flexural Deformation by the Adjacent Beam and Column Webs [17]

Figure 4 : Joint moment contributed by various surrounding elements.

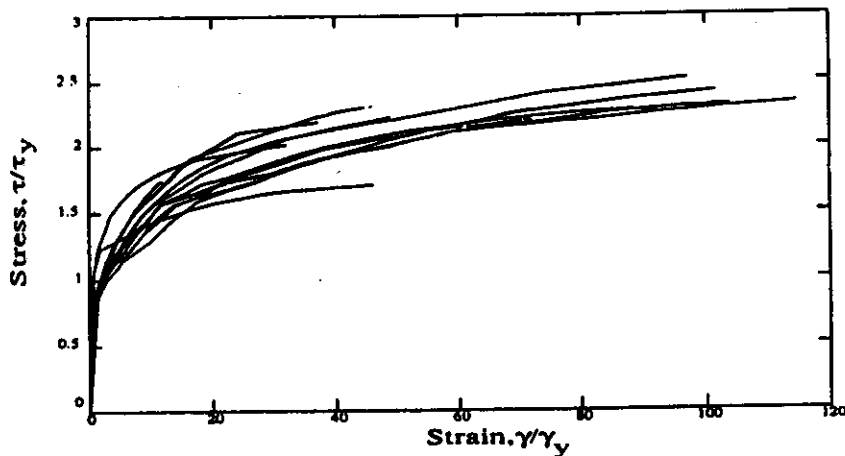


Figure 5 : Summary of the experimental data (Kato, 1982) of the monotonic stress-strain curves of the joint shear responses from steel beam-column sub-assembly tests.

(Kato, 1982) offered by the adjacent beam and column webs (see Fig. 4c), and (d) strain hardening of the panel zone plate.

The monotonic load-deformation curves for the shear response of joints, obtained from numerous experimental research projects (Kato, 1982), are shown in Fig. 5. The well-defined knee in the early inelastic regime, is a significant feature of all these tests. The yielding of the joint is found to occur before the theoretical yield shear is reached at about 0.8 times the yield shear stress (Krawinkler & Popov, 1982). This is attributed to the combined action of the factors contributing to the shear stiffness discussed above. The joint shows a remarkable increase in strength beyond yield. Its post-yield stiffness is noteworthy over a long range of inelastic deformation upto about 100 times the yield shear strain, and so exhibits a remarkable amount of ductility. Further, under cyclic loading, repetitive hysteresis loops are observed for its shear behaviour with no drop in strength even under very large inelastic joint distortions. Thus, the joint demonstrates excellent stable energy dissipating characteristics.

#### The Joint Hysteresis Model

In the literature, there are a number of analytical models (Pinkney, 1973; Krawinkler *et. al.*, 1975; Kato, 1982; Fielding & Chen, 1973) describing the hysteretic behaviour of beam-column joints. They are reasonable approximations, but can be improved in several ways. The ultimate load is underestimated in the Krawinkler-Popov Model (Krawinkler & Popov, 1982). The post-yield joint stiffness is applicable only over a small range of inelastic behaviour, *i.e.*, only up to 4 times the yield strain. The Kato Model (Kato,

1982), overcomes this difficulty by defining the virgin curve over a larger range of inelastic behaviour, but it uses a multi-linear virgin curve. The Fielding-Chen Model (Fielding & Chen, 1973) uses a simplified bi-linear virgin curve, which over-estimates the post-yield stiffness.

Recently, a simple semi-empirical model was proposed (Murty, 1992) for the hysteretic behaviour of beam-column joints. It is convenient for numerical implementation, even under cyclic loading. This *Ellipsoidal Joint Hysteresis Model* can be used in the analysis of steel planar moment-resisting frames. This model is based on the summary (shown in Figure 6) of the monotonic test data (Kato, 1982) on panel zones. The model empirically defines a virgin curve for the joint hysteresis behaviour, as shown in Fig.7, which is essentially a function of  $M_y$  and  $\gamma_y$ . Further, the hysteresis loops or the branch curves, are defined by cubic ellipses, as shown in Fig.8. In Fig.9, a typical experimental joint hysteresis loop (Krawinkler et. al., 1975) is shown along with the corresponding analytical prediction. These comparisons show a close agreement to the experimental data. The model employs a set of rules to define the cyclic response of structural steel joints (Murty, 1992).

The Ellipsoidal Joint Hysteresis Model for steel beam-column joints in moment-resisting plane frames is significantly superior to the currently used models. This model is based on the macroscopic view of the overall joint behaviour and is supported by test data from steel beam-column sub-assemblages. It provides smooth and explicit expressions for joint moment in terms of the shear strain. The few non-cumbersome hysteretic rules make the model simple and computationally efficient, yet descriptive enough to adequately represent the features of real hysteretic behaviour. The smooth virgin curve, and a realistic estimate of the ultimate capacity and the possible inelastic range of the joint, are the strengths of this model. With hysteretic behaviour defined up to  $100 \gamma_y$ , this model is an excellent choice for the analytical modelling of structural steel beam-column joints.

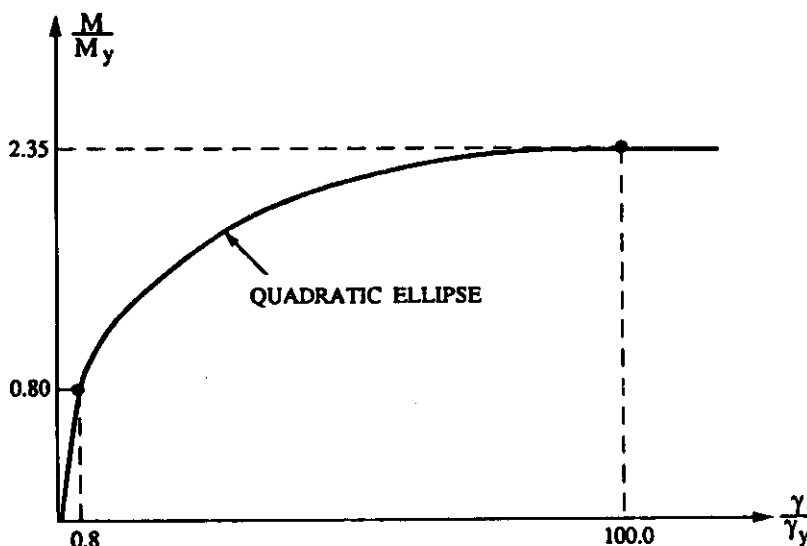


Figure 6 : Joint moment vs joint shear strain curve used as the backbone curve in the Joint Hysteresis Model.

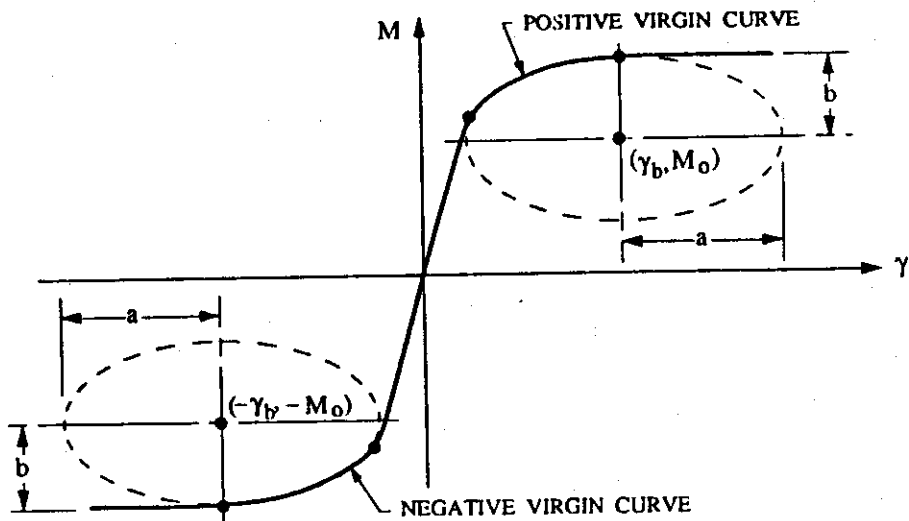


Figure 7 : Geometry of the quadratic ellipses modelling the nonlinear virgin curve in the Joint Hysteresis Model.

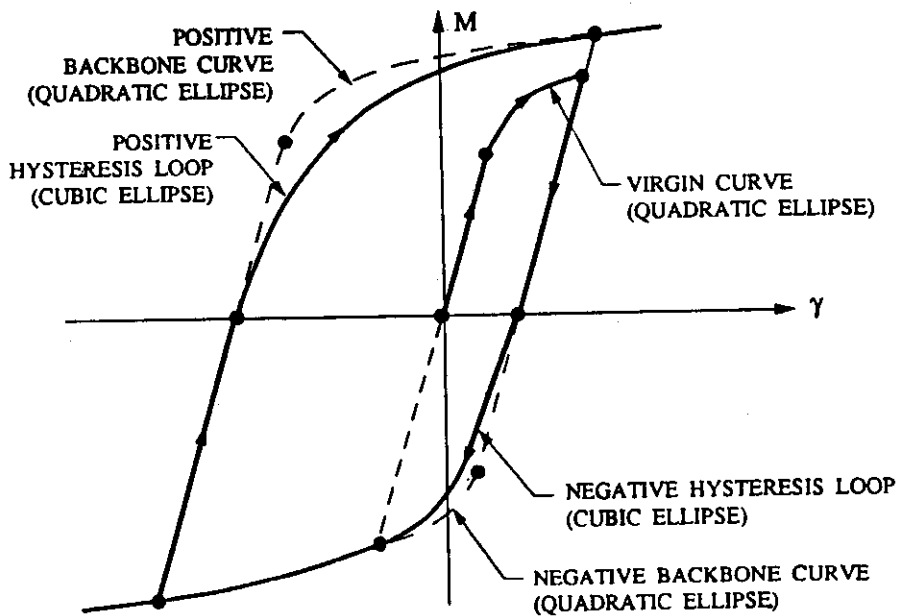


Figure 8 : Quadratic ellipses for virgin curves and backbone curves, and cubic ellipses for positive and negative hysteresis loops in the Joint Hysteresis Model.



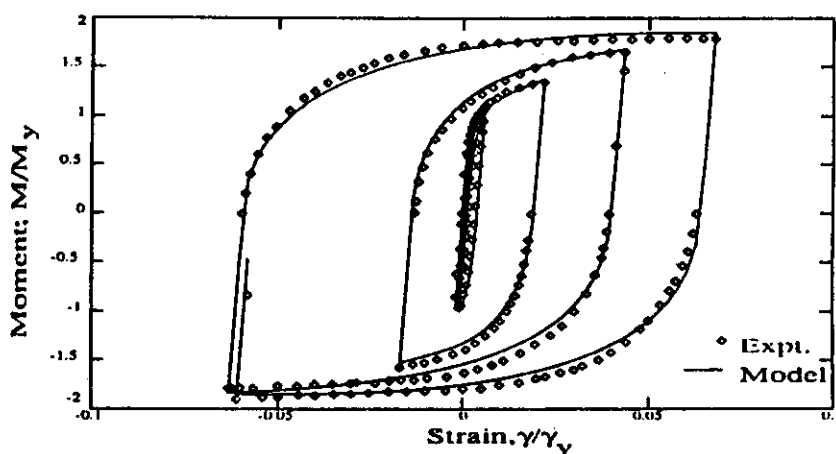


Figure 9 : Comparison of experimental hysteresis loops (Krawinkler et. al., 1975) of the shear response of a steel joint from the sub-assembly test, with theoretical prediction using the Joint Hysteresis Model.

## MODELLING OF BUILDINGS

A building frame may be discretised into a finite number of beam-columns inter-connected through the joints. Since finite sizes of the joints are considered, clear spans are used for the beam-columns. Also, since the joints have finite size and stiffness, separate joint elements discussed above, are used in the modelling of the frame.

The deformed geometry of a structure leads to a redistribution of the internal forces within its components, which could be very significant. Hence, this effect of large deformations in a frame is included through nodal updating. Also, the inelastic effects introduced through the material constitutive law are included. This non-linearity introduces a stable form of energy dissipation through hysteretic response of the material. The input seismic energy is dissipated through this mechanism.

### Degrees of Freedom

The physical idealisation of a joint in a planar MRF is shown in Fig.10. At each node of the natural global discretisation, i.e., at the junctions of beams and columns, a plane frame with joint elements has four degrees of freedom, namely two in-plane translations, beam rotation and column rotation (see Fig.11). A beam column has six exterior degrees of freedom (see Fig.12a), and a joint element has two degrees of freedom, namely beam rotation,  $\mu$ , and column rotation,  $\nu$  (see Fig.12b). The shear strain in the joint is given by

$$\gamma = \mu - \nu. \quad (1)$$

If  $\Delta\mu$  is incremental joint rotation vector and  $\Delta m$  is incremental joint moment vector, then the linearised incremental equation of joint panel is

$$K_t^J \Delta\mu = \Delta m, \quad (2)$$

where  $K_t^J$  is the tangent stiffness matrix of the joint.

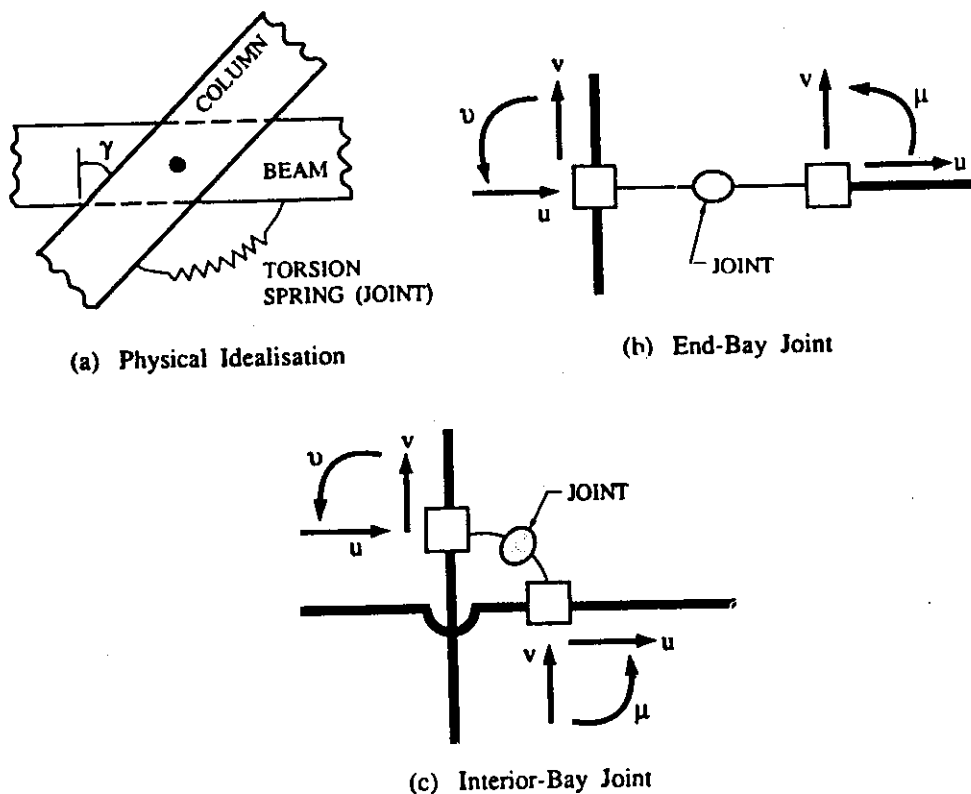


Figure 10 : Physical idealisation of a joint and the degrees of freedom at a typical node of a planar frame.

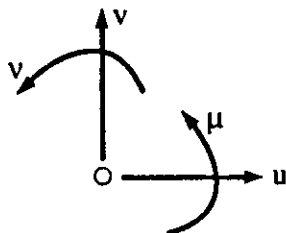


Figure 11 : Global degrees of freedom at each node of a planar frame.

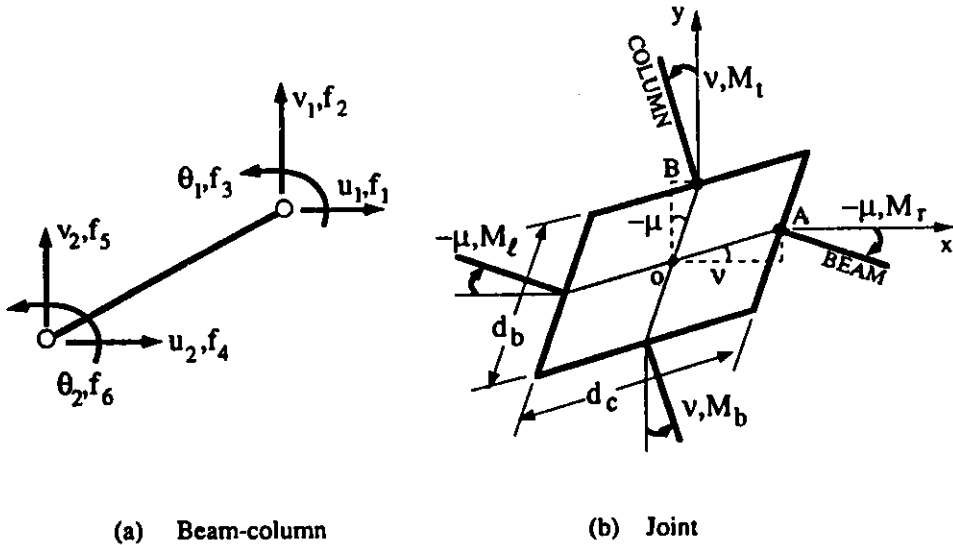


Figure 12 : Global degrees of freedom of beam-column and joint elements.

#### Incremental Equation of Motion

The nonlinear dynamic equilibrium equation of the frame at time  $t$  is

$$M \underline{\ddot{x}}(t) + C \underline{\dot{x}}(t) + \underline{p}(\underline{x}, t) = \underline{f}(t), \quad (3)$$

where  $\underline{x}(t)$ ,  $\underline{\dot{x}}(t)$  and  $\underline{\ddot{x}}(t)$ , respectively, are its displacement, velocity and acceleration relative to the ground.  $\underline{p}(\underline{x}, t)$  represents the stiffness forces produced in the frame under the application of external forces,  $\underline{f}(t)$ , comprising of the constant gravity loads,  $\underline{f}_0$ , and the time-dependant lateral inertia forces,  $\underline{f}_g(t)$ . The nonlinear response quantities,  $\underline{x}(t)$ ,  $\underline{\dot{x}}(t)$  and  $\underline{\ddot{x}}(t)$  at time  $t$ , are obtained by the direct integration of Eq. (3) in the time domain. Since, Eq. (3) is nonlinear, the Modified Newton Raphson Method in conjunction with the Newmark's  $\gamma$ - $\beta$  Method is normally used. Eq. (3) can be re-written as

$$\begin{aligned} & \left[ \beta K_e + \frac{\gamma}{\Delta t} + \frac{1}{(\Delta t)^2} M \right] \Delta \underline{x}^k \\ &= \beta \underline{f}(t + \Delta t) - \beta \underline{p}^k(t + \Delta t) \\ & - \left[ \frac{\gamma}{\Delta t} C + \frac{1}{(\Delta t)^2} M \right] \underline{x}^k(t + \Delta t) + \left[ \frac{\gamma}{\Delta t} C + \frac{1}{(\Delta t)^2} M \right] \underline{x}(t) \\ & + \left[ (\gamma - \beta) C + \frac{1}{\Delta t} M \right] \underline{\dot{x}}(t) + \left[ (\gamma - 2\beta) \frac{\Delta t}{2} C + (0.5 - \beta) M \right] \underline{\ddot{x}}(t) \end{aligned} \quad (4)$$

Eq. (4) is solved by the Gauss Elimination Procedure to obtain the incremental displacements (or deformation) in iteration  $k$ ,  $\Delta \underline{x}^k$ , within the load step. Using this updated incremental displacement vector,  $\Delta \underline{x}^k$ , the states of all

members and joints are updated, and the revised  $\underline{p}^{k+1}(t+\Delta t)$  vector is obtained. The iterations are continued until the residual force vector is within the tolerance.

#### Obtaining $\underline{p}^{k+1}(t+\Delta t)$ Vector

The cumulative global nodal incremental displacement vector,  $\Delta \underline{x}$ , is

$$\Delta \underline{x} = \underline{x}^{k+1}(t+\Delta t) - \underline{x}(t), \quad (5)$$

where

$$\Delta \underline{x}^{k+1}(t+\Delta t) = \underline{x}^k(t+\Delta t) + \Delta \underline{x}^k.$$

$\Delta \underline{x}$  is used to form individual global incremental end-displacement vector,  $\Delta \underline{u}^m$ , of member  $m$ , whether a beam-column or a joint, using connectivity information.  $\Delta \underline{u}^m$  is applied to the state of member  $m$  at the start of the previous time step, and the updated geometry is obtained by nodal coordinate updating. The updated global end-force vector,  $\underline{f}^m$ , of member  $m$  is obtained using its constitutive stiffness relations. The global member end-force vectors of beam-column and joint elements are then assembled to obtain the  $\underline{p}^{k+1}(t+\Delta t)$  vector for the whole frame. This is used in Eq.(4) in iteration  $(k+1)$ .

#### Numerical Implementation of Joint Characteristics

The numerical implementation of the joint element is very simple. In nonlinear analysis, the two most important steps are associated with the computation of the elastic stiffness of the joint and with the updating of the joint force vector after each load step.

**Elastic Joint Stiffness :** The joint elastic shear stiffness,  $J_{K_e}$ , is

$$J_{K_e} = \frac{M_y}{\gamma} = G d_c d_b t \quad (6)$$

Since this stiffness is associated with the shear strain,  $\gamma$ , of the joint, the elastic stiffness matrix of the joint, in terms of the two joint global degrees of freedom, the beam rotation,  $\mu$ , and the column rotation,  $\nu$ , becomes

$$K_e^J = \begin{bmatrix} J_{K_e} & -J_{K_e} \\ -J_{K_e} & J_{K_e} \end{bmatrix} \quad (7)$$

The linear equilibrium equation of the joint is

$$\begin{Bmatrix} M_\mu \\ M_\nu \end{Bmatrix} = \begin{bmatrix} J_{K_e} & -J_{K_e} \\ -J_{K_e} & J_{K_e} \end{bmatrix} \begin{Bmatrix} \mu \\ \nu \end{Bmatrix}, \quad (8)$$

where  $M_\mu$  and  $M_\nu$  are the sum of the beam and column moments, respectively, as shown in Fig.12. In Eq.(8),  $J_{K_e} = G d_c d_b t$ , where  $G$  is the shear modulus, and  $d_c$ ,  $d_b$ ,  $t$  are the joint panel dimensions. Eq.(8) is not valid for inelastic joint deformation. However, the iterating stiffness of the structure does not require such a relation (Murty, 1992).

**Joint Force Vector :** At the end of each global iteration within a load step, the incremental joint displacement vector,  $\Delta \underline{u}^n$  is given and the updated joint stiffness force vector,  $\underline{f}^n(t+\Delta t)$  is required. This is obtained directly from the hysteresis rules in the Ellipsoidal Joint Hysteresis Model (Murty, 1992) using  $\Delta \underline{u}^n$  and  $\underline{f}^n(t)$ .

### SEISMIC ENERGY DISSIPATION

In accordance with the seismic design philosophy, a structure is designed for a much less base shear force than what would be experienced if it were to remain elastic during the most severe shaking likely at that site. Here, ductility and overstrength of the structure are relied upon to compensate for reduced level of design base shear (Jain, 1994; Navin & Jain, 1993; Rashad, 1993).

Buildings experience inelastic ductile behaviour under large events. They need to dissipate seismic energy through inelastic hysteretic dissipation without any collapse. For this, the stiffness, strength and overstrength of the structure must be so chosen that a minimum and a maximum required ductilities is ensured in it during these large, but rare, events (Uang & Bertero, 1988; Popov et. al., 1993). Minimum ductility is required to ensure a reduced design base shear, while maximum ductility is required to restrict the overall drift, and hence the damage, in the building.

One efficient way of controlling ductility is through the design of the joint panel zones. The strength and stiffness of the joint directly influence the ductility and drift, respectively, of the frame. However, ductility and drift are inter-related. Hence, there exists an optimal design of joints which limits the maximum drift, ensures a minimum ductility and maximizes the hysteretic energy dissipation capacity.

### Frame Sub-Assemblage

Buildings primarily respond in lateral shear. Hence, a study of the lateral load-deformation history under cyclic loads indicates its energy dissipation capacity. Further, since the overall drift of the building is contributed by the individual storey drifts, it is adequate to study the characteristic of a typical storey sub-assemblage alone. The quantities that need to be studied while estimating the contribution of a storey sub-assemblage to the inelastic energy dissipation of the frame, are storey-shear and storey-drift.

### Panel Zone Designs

To study this, consider a typical storey sub-assemblage of a three-bay planar frame as shown in Fig.13. The following four options may be considered insofar as the design of joint panel zones for steel frames are concerned.

**Design J1 :** Joints are designed to be weak. The thickness of the joint panel zone plate,  $t_j$ , is chosen to be the same as the thickness of the column web,  $t_{cw}$ , i.e., no doubler plates are added. Hence,

$$t_j = t_{cw}.$$

(9)

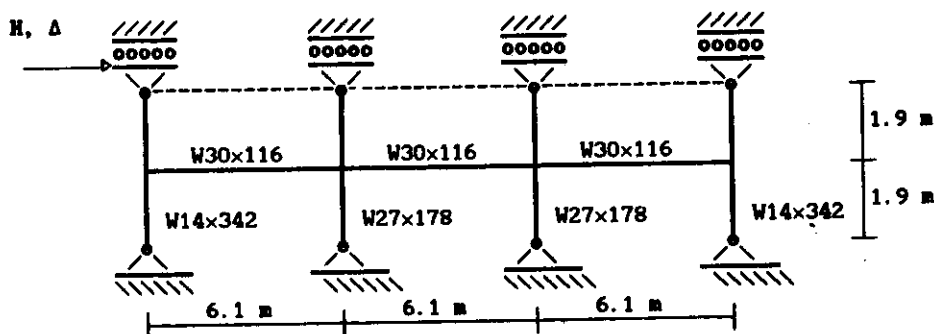


Figure 13 : Typical Storey Sub-Assemblage within a 3-bay Planar Frame showing the Storey Shear,  $H$ , and Storey Drift,  $D$ .

The panel zones are based on the code (UBC 1991) designed beam and column sizes. This is a lower bound for the design of panel zones.

**Design J2 :** Joints are designed as per UBC 1991. The thickness of the joint panel zone plate is determined by :

$$t_j = \frac{0.8 \sum (M_p)_{bj}}{\tau_y d_b d_c} \quad (10)$$

where  $\tau_y = \sigma_y / \sqrt{3}$ . In Eq. (10),  $\sum (M_p)_{bj}$  refers to the sum of plastic moment capacities of all beams framing into that joint.  $\sigma_y$  is the yield stress. If  $t_j$  is less than  $t_{cw}$ , then the latter is used. Here, the panel zone need not allow the formation of hinges in beams to make the frame ductile. Hence, the ductility demands on the beam-column members are reduced. This is the upper-bound design suggested in UBC 1991.

**Design J3 :** Joints are designed to be very strong. The thickness of the joint panel zone plate is determined by :

$$t_j = \frac{1.5 \sum (M_p)_{bj}}{\tau_y d_b d_c} \quad (11)$$

The factor 1.5 accounts for the strain-hardening of adjoining beam moments over their plastic moment capacities and for ensuring that the linear elastic range of the joint is not exceeded. Again, if  $t_j$  is less than  $t_{cw}$ , then the latter is used. Here, the panel zones are relieved of ductility demands by designing them to remain elastic, by setting their yield strength at an arbitrary large value. This design incorporates only the stiffness of flexible joints, and restricts yielding to girders and columns only.

**Design G :** The girders are designed to be very strong, so that no hinges are formed in them. However, the joints are as per design J1.

#### Discussions

For the storey sub-assemblage shown in Figure 13, typical storey shear vs storey drift curves for one complete cycle for the four joint designs indicated above are given in Figure 14. Clearly, the energy dissipated in

design J1 is substantially larger than that from the other designs. Frame ductility distribution between the joints, beams and columns can be controlled through the design of the joints or through the design of beams. Stronger joints throw more ductility demands on the columns, and the weaker joints attract the ductility towards themselves. However, weak joints may not perform well under ground motions with displacement jumps (Murty, 1992). Thus, when the girders are strong, i.e., the hinges are formed only in the joints, the drift is observed to be lesser than in the case where both girders and joints are weak, but the energy dissipation is reduced. This suggests that one needs to balance the girder strength in such a way that the energy dissipation is maximized while keeping the drift within the limits.

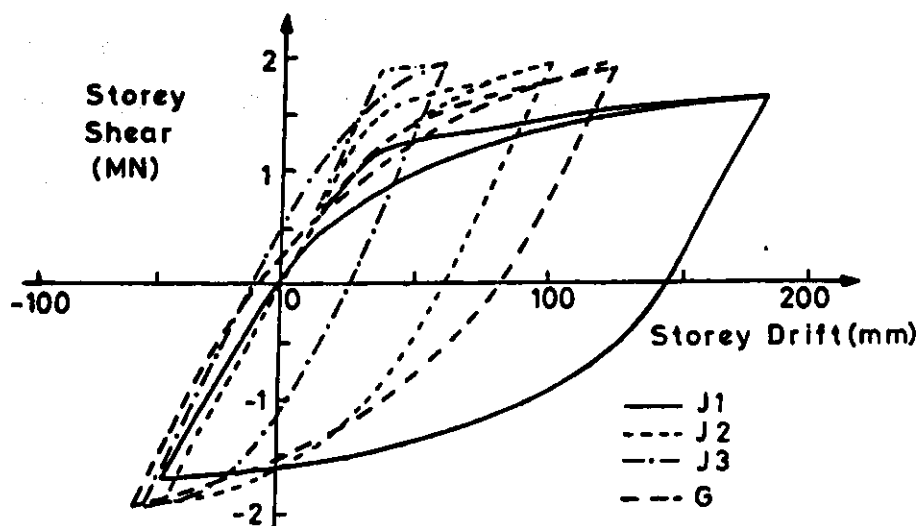


Figure 14 : Typical Storey Shear vs Storey Drift Behaviour for Different Frame Designs

It is obvious that the joints have a finite strength and carry the lateral load till such time its capacity is reached. After that, they undergo large inelastic deformations. Clearly, joint panel zones dissipate seismic energy in a stable manner in the inelastic region.

#### SUMMARY

This paper highlights the advantage of using frame joints as controllers of the input seismic energy dissipation. A strong need is felt to further investigate the optimum proportions of beam-column and joint elements. The current design philosophy of "strong-column, weak-girder" may have to be replaced. A new philosophy of "strong-column, weak-girder, weaker-joint" has great promise in the design of steel frames with a view to releasing seismic energy in a stable manner. More research is required to arrive at specific design provisions.

## REFERENCES

1. Becker, R. (1975), "Panel Zone Effect on the Strength and Stiffness of Steel Rigid Frames," *AISC Engineering Journal*, No. 1, pp 19-29.
2. Bertero, V.V., Popov, E.P., and Krawinkler, H. (1972), "Beam-Column Sub-Assemblages under Repeated Loading," *ASCE JI. of the Structural Division*, Vol. 98, No. ST5, pp 1137-1159.
3. Chen, W.F., and Atsuta, T. (1977), *Theory of Beam-Columns*, Vols.: 1 and 2, McGraw-Hill International Book Company, Inc., New York.
4. Fielding, D.J., and Chen, W.F. (1973), "Steel Frame Analysis and Connection Shear Deformation," *ASCE JI. of the Structural Division*, Vol. 99, No. ST1, pp 1-18.
5. Jain, S.K., *Seismic Analysis and Design* (under publication).
6. Kato, B. (1982), "Beam-to-Column Connection Research in Japan," *ASCE JI. of the Structural Division*, Vol. 108, No. ST2, pp 343-360.
7. Krawinkler, H. (1978), "Shear in Beam-Column Joints in Seismic Design of Steel Frames," *AISC Engineering Journal*, No. 3, pp 82-91.
8. Krawinkler, H., and Popov, E.P. (1982), "Seismic Behaviour of Moment Connections and Joints," *ASCE JI. of the Structural Division*, Vol. 108, No. ST2, pp 373-391.
9. Krawinkler, H., Bertero, V.V., and Popov, E.P. (1971), "Inelastic Behaviour of Steel Beam-to-Column Subassemblages," *Report No.: UCB/EERC 71-7*, University of California, Berkeley.
10. Krawinkler, H., Bertero, V.V., and Popov, E.P. (1975), "Shear Behaviour of Steel Frame Joints," *ASCE JI. of the Structural Division*, Vol. 101, No. ST11, pp 2317-2334.
11. Murty, C.V.R. (1992), "Nonlinear Seismic Response of Steel Planar Moment-Resisting Frames," *Report No.: EERL 92-01*, California Institute of Technology, Pasadena.
12. Nakao, M. (1973), "Experiment of the Behaviour of Steel Beam-to-Column Connections with Large Axial Force of Column," *Annual Report of Engineering Research Institute*, University of Tokyo, Tokyo, Japan, Vol. 32.
13. Navin, R., and Jain, S.K. (1993), "Assessment of Seismic Overstrength in Reinforced Concrete Frames," *Research Report*, Department of Civil Engineering, I.I.T. Kanpur, Kanpur, India.
14. Pinkney, R.B. (1973), "Cyclic Plastic Analysis of Structural Steel Joints," *Report No.: UCB/EERC 73-15*, University of California, Berkeley.
15. Popov, E.P., Yang, T.-S., and Grigorian, C.E., "New Directions in Structural Seismic Design," *Earthquake Spectra*, Journal of the Earthquake Engineering Research Institute, California, Vol. 9, No. 4, pp 843-876.
16. Rashad, G.E.-E. (1993), "A Ductility and Displacement Based Design Procedure for Seismic Design of Reinforced Concrete Frames," *Ph.D. Thesis*, Department of Civil Engineering, I.I.T. Kanpur, Kanpur.
17. Tsai, K.-C., and Popov, E.P. (1988), "Steel Beam-Column Joints in Seismic Moment Resisting Frames," *Report No.: UCB/EERC 88-19*, University of California, Berkeley.
18. Uang, C.-M., and Bertero, V.V. (1988), "Implications of the Recorded Earthquake Ground Motions on Seismic Design of Building Structures," *Report No.: UCB/EERC 88-13*, Earthquake Engineering Research Centre, University of California, Berkeley.
19. *Uniform Building Code* (1991), International Conference of Building Officials, Whittier, California.

. . . . .